# Molten-Salt Closed-Loop Geothermal Systems for Super-Hot Rock Resources: Thermal Drawdown Mitigation and Dispatchable Power through Thermal Buffering

David Alan McBay, Ajan Meenakshisundaram, Ramsey Doueiri, Yoshitake Yamaguchi, Ron Swenson, Wildani Putra, Thomas McBay

**Keywords:** Super-hot rock geothermal, closed-loop geothermal systems, molten salt heat transfer, thermal drawdown mitigation, geothermal thermal energy storage, coaxial well heat exchangers (concentric geometry)

**ABSTRACT**

This paper presents a molten-salt closed-loop geothermal system developed primarily for super-hot rock environments, where subsurface temperatures exceed those typically accessible to conventional hydrothermal technologies. By operating at ultra-high temperatures and employing molten salt as both the subsurface heat-transfer fluid and the surface thermal storage medium, the system enables efficient, dispatchable geothermal power generation without formation fluid production or reservoir pressure depletion. The paper focuses on the thermodynamic advantages of super-hot rock operation, engineering strategies for mitigating thermal drawdown, and the role of molten-salt thermal buffering in improving system longevity and project economics. Secondary deployment pathways, including retrofits of existing geothermal wells and selected orphaned oil and gas wells, are discussed as complementary but non-primary applications.

## 1. INTRODUCTION

Super-hot rock geothermal resources represent one of the largest underdeveloped sources of firm, zero-carbon energy. At temperatures commonly exceeding 400 °C, these resources offer the potential for significantly higher power density and conversion efficiency than conventional geothermal systems. However, their development has historically been limited by drilling challenges, material constraints, and concerns regarding long-term thermal sustainability. (Ref. [12] Colp., 1982)

Closed-loop geothermal systems provide a fundamentally different approach by eliminating formation of fluid production and decoupling energy extraction from reservoir pressure behavior (Ref. [7] Meenakshisundaram et al., 2024). When combined with molten salt as the heat-transfer medium, closed-loop systems become well suited for super-hot rock environments, where high thermal stability and large temperature differentials are essential. This paper examines the technical foundations of molten-salt closed-loop geothermal systems with a primary focus on super-hot rock deployments, addressing thermal drawdown concerns and demonstrating how thermal buffering enables dispatchable, economically robust power generation.

### 1.1. Closed-loop geothermal systems as thermally governed energy systems

The instantaneous thermal power extracted from the subsurface is determined by the mass flow rate of the working fluid and the temperature difference between the inlet (injection) and outlet (production).

Thermal power (Ref. [2] Ali et al., 2019)

$$P_{th} = m * C_p * (t_2 - t_1)$$

(1)

where $P_{th}$, $m$, $C_p$, $t_2$ and $t_1$ are thermal power, mass flow rate, specific heat capacity of the fluid, outlet (production) temperature, and inlet (injection) temperature, respectively.

Net electrical power (Ref. [2] Ali et al., 2019)

$$P_{net} = (P_{th} * \eta_c) * (P_p)$$

(2)

Where $P_{net}$, $P_{th}$, $\eta_c$, and $P_p$ Are net power, net thermal power, cycle efficiency, and pump power, respectively.

$$P_p = V \times (P_2 - P_1) / (\eta P)$$

(3)

McBay, Meenakshisundaram, Doueiri, Yamaguchi, Swenson, Putra, McBay

where $P_p$, V, $P_1$ and $P_2$ are pump power, volumetric flow rate, inlet and outlet pressure, and pump efficiency, respectively. System efficiency (Ref. [3] Zarrouk et al., 2014).

$$H = W_{net}/Q_{in} \tag{4}$$

$$W_{net} = W_t - W_p \tag{5}$$

$$W_t = (m*(h_2-h_1)) \tag{6}$$

$$W_{p=}(m*v*\Delta p/\eta p) \tag{7}$$

Where $W_{net}$, $Q_{in}$, $W_p$, $W_t$, $h_1$, and $h_2$ are net work, heat input rate, pump work, total work, and inlet and outlet enthalpy, respectively.

For the thermal power estimate in Eq. (1), the inlet (injection) temperature is assumed to $T_1 = 150°C$ and the outlet (production) temperature is $T_2 = 500°C$, corresponding to a temperature increase of $\Delta T = 350°C$.

**Table 1: System parameters estimation for a closed loop molten salt geothermal system.**

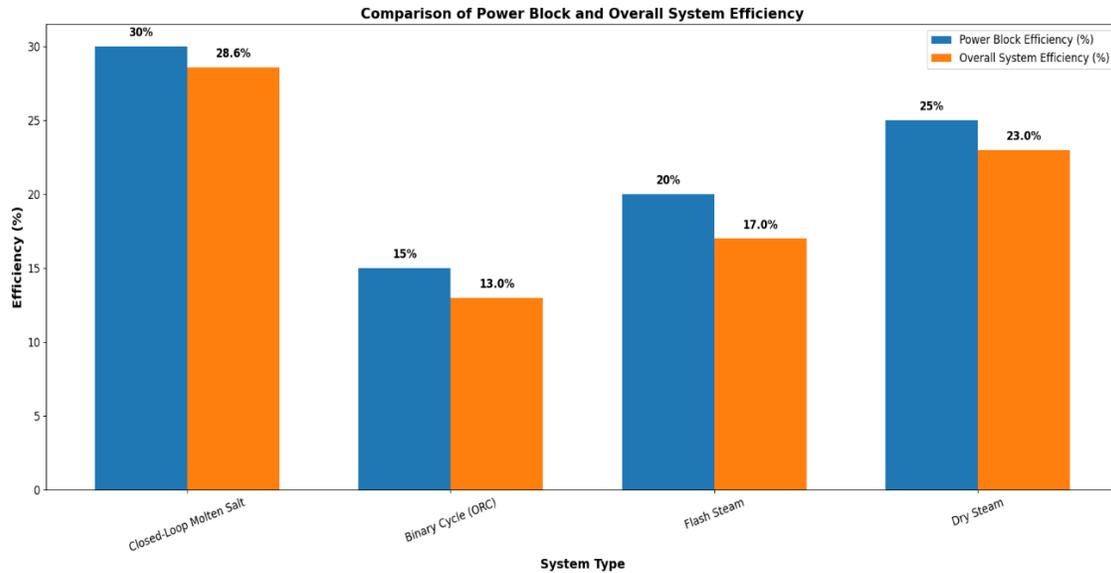| Parameter | Value | Units |
|---|---|---|
| Thermal Power Extracted ($Q_{th}$) | 42,438 | kW |
| Pump Power Consumption | 587 | kW |
| Pump Efficiency | 70 | % |
| Power Block Efficiency (ORC) | 30 | % |
| Gross Electrical Power Output | 12,731 | kW |
| Net Electrical Power Output | 12,145 | kW |
| Net Thermal Power Extracted | 42,438 | kW |
| System Net Efficiency | 28.6 | % |
| Parasitic Loss | 4.6 | % |

**Figure 1: Comparison of Organic Rankine Cycle (ORC) power block and overall system efficiency between various geothermal systems.**

The bar chart above compares the power block efficiency and overall net system efficiency for four different geothermal power system types. The closed-loop molten salt system exhibits the highest performance, achieving a power block efficiency of 30% and an overall system efficiency of 28.6%, reflecting high operating temperatures and low parasitic losses (Ref. [6] McBay., 2012). Binary Cycle (ORC) systems show the lowest efficiencies due to lower operating temperatures and higher parasitic consumption. Flash steam systems demonstrate moderate efficiency, while dry steam systems approach high performance, with efficiencies close to those of the closed-loop molten salt system. Overall, the plot highlights the strong efficiency advantage of high-temperature systems with minimized parasitic losses.

### 1.2. Ten-Megawatt Super-Hot Pilot Project as a Working Field Model

Clean Air Task Force mapping indicates that many regions already possess super-hot rock geothermal conditions suitable for immediate deployment of molten-salt closed-loop systems. Numerous existing geothermal and petrothermal wells exceed 375 °C at depths below 5 km, including wells at Japan's Kakkonda field with measured temperatures approaching 580 °C at depths under 4 km. Similar conditions occur globally at depths compatible with commercial drilling. Where suitable high-temperature wells exist and offtake is available, new drilling is unnecessary.

The objective of the initial project is to establish a commercially operating field model rather than a scientific test well. Scalable geothermal deployment requires demonstration of safe, predictable, and profitable operation. The pilot is therefore designed using existing data, proven materials, and commercially available equipment, with revenue generation beginning at first operation. Operational and subsurface data are collected as part of routine commercial performance.

The pilot is defined as a 10 MW molten-salt closed-loop system operating in super-hot rock. Development requires either an existing well exceeding 375 °C at less than 5 km depth or a newly drilled well meeting the same criteria if necessary. Long-term offtake is secured through a 20-year power purchase or equivalent heat contract. Project cost is approximately US $30 million when an existing well is used, with additional cost only if new drilling is required. The project may be sited in jurisdictions with supportive regulation, reliable offtake, and no sanction constraints.

Successful operation of a revenue-generating super-hot pilot establishes the technical and economic basis for scaling molten-salt closed-loop geothermal. Demonstration of dispatchable, ultra-high-temperature operation is essential for attracting large-scale private investment.
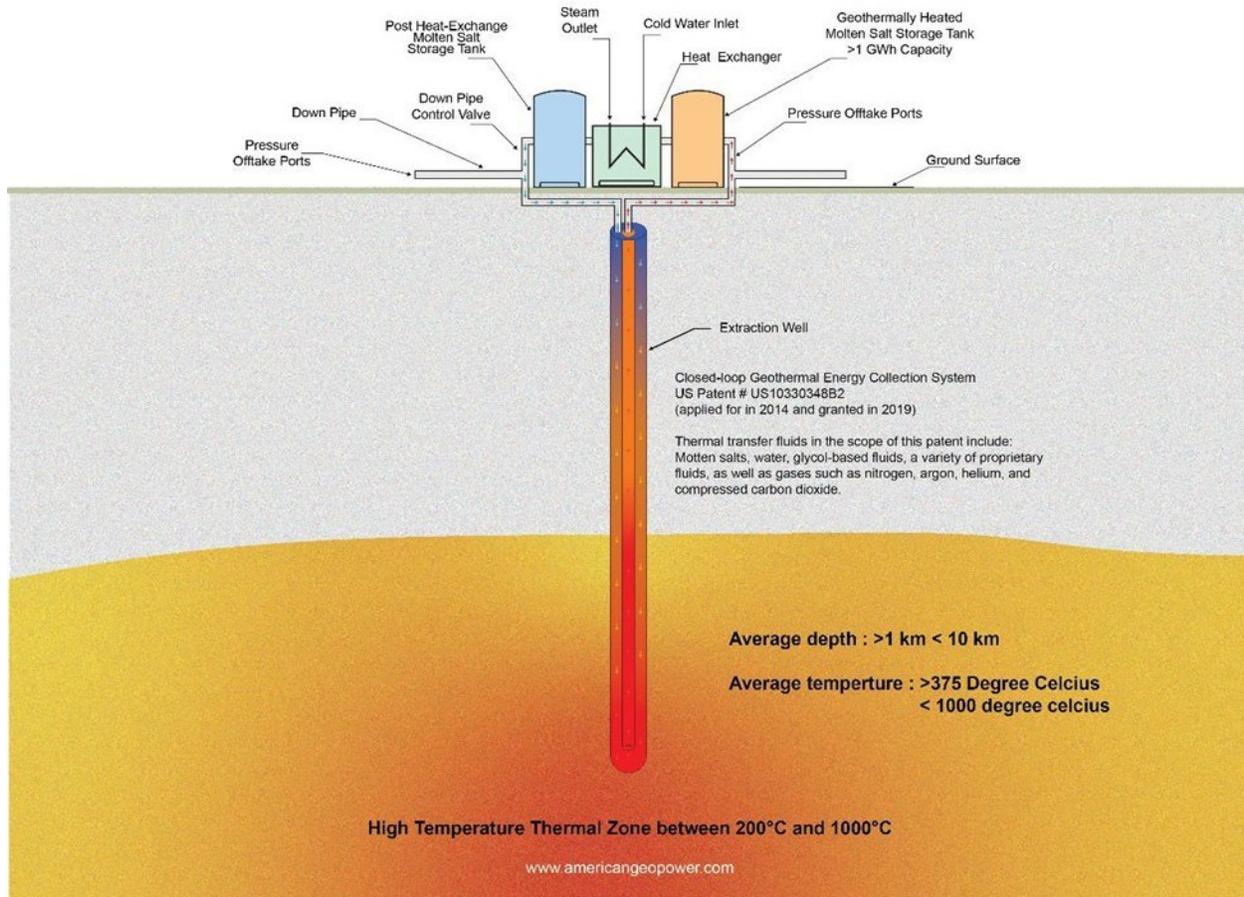
**Figure 2: Coaxial Super High Temperature Closed Loop Geothermal System.**

## 2. SYSTEM ARCHITECTURE FOR SUPER-HOT ROCK CLOSED-LOOP GEOTHERMAL

The proposed system employs a sealed closed-loop architecture in which molten salt circulates through a coaxial (concentric) well drilled into super-hot rock formations. Heat is transferred conductively from the surrounding rock into the molten salt and transported to the surface for power conversion and thermal storage.

The system is designed for sustained ultra-high-temperature operation while maintaining predictable heat extraction rates. Flow control, materials selection, and thermal insulation are optimized to minimize internal losses and preserve strong formation-to-fluid temperature gradients. While adaptable to existing wellbores, the architecture is primarily intended for new wells drilled specifically to access super-hot rock resources (Ref. [13] CATF., 2022).

To maximize heat capture and ensure durability, the first commercial system employs a hybrid downhole materials strategy matched to local thermodynamic conditions along the well column (Ref. [14] Special Metals Corporation., 2005). In the deepest high-temperature interval, super-high-temperature alloys such as Inconel or Hastelloy provide high thermal conductivity, corrosion resistance, and mechanical strength at temperatures approaching 550 °C, enabling rapid conductive heat transfer into the circulating molten salt. In the upper sections, where heat preservation is critical, the system transitions to vacuum-insulated tubing (VIT), validated for operation up to 500 °C, to minimize conductive, convective, and radiative losses as the molten salt returns to the surface (Ref. [16] Vallourec THERMOCASE® VIT., tech sheet, no date). This integrated materials approach improves efficiency, protects system integrity, and enables reliable energy delivery from super-hot rock environments.

## 3. THERMAL DRAWDOWN IN CLOSED-LOOP GEOTHERMAL SYSTEMS

Thermal drawdown refers to the reduction in formation temperature adjacent to a heat-extraction interface over time. In closed-loop geothermal systems, drawdown is governed by conductive heat transfer within the surrounding rock rather than by fluid depletion or

pressure decline. Consequently, drawdown behavior depends on heat-flux density, formation thermal properties, and the spatial distribution of heat-exchange surfaces.

From a physics perspective, the core advantage of a sealed closed-loop system is that long-term performance is governed primarily by conductive heat replenishment in the surrounding rock, rather than by reservoir pressure decline or formation-fluid depletion. To first order, the thermal power delivered to the working fluid is set by Fourier conduction,

$$Q \approx kA\frac{\Delta T}{L}$$

(8)

where Q is the heat transfer rate, and k is the effective rock thermal conductivity, A is the effective heat-exchange area, $\Delta T$ is the formation-to-fluid temperature difference, and L is the characteristic conduction length scale. In super-hot rock settings, the large $\Delta T$ allows a target $\dot{Q}$ to be achieved at lower heat-flux density ($\dot{Q}/A$), which directly reduces near-well thermal gradients and mitigates localized thermal drawdown.

Thermal drawdown itself can be framed as a classical heat-diffusion problem. The relevant timescale for conductive replenishment scales as

$$t_{diff} \sim \frac{L^2}{\alpha}$$

(9)

with thermal diffusivity $\alpha = k/(\rho c)$. This highlights why geometry and operating strategy matter: increasing the effective A (e.g., via multilateral/interconnected exchange surfaces) and controlling L (i.e., distributing extraction over a larger rock volume) can keep the system within a favorable diffusion regime over commercial lifetimes.

In super-hot rock environments, the magnitude of available sensible heat and large temperature gradients provide inherent advantages for long-term heat extraction. However, without deliberate control of heat-exchange geometry and operating conditions, localized cooling can still occur. Addressing thermal drawdown is therefore a design and operational requirement rather than an inherent limitation of closed-loop geothermal systems.

### 3.1. Governing heat transfer physics in host formation

This equation represents transient radial heat conduction in the surrounding rock of a geothermal reservoir. It relates the temporal change in rock temperature to radial heat diffusion governed by the rock's thermal conductivity, density, and specific heat capacity, describing how heat propagates outward from the wellbore over time. Equation (Radial, 1D simplification near the wellbore) (Ref. [1] Hefani et al., 2021):

$$Pr*cp,r(\partial T/\partial t) = 1/r*\partial/\partial r(kr*\partial T/\partial r) \tag{10}$$

Heat is carried away by the molten salt and represented by convective heat transfer coefficient. The heat extraction per unit length of the wellbore.

$$Q = h*a*(T_w - T_b) \tag{11}$$

- $\dot{Q}$ = Heat transfer rate [W]

- h = Convective heat transfer coefficient [W/m²·K]

- a = Heat transfer surface area [m²] = $\pi DL \pi DL$

- $T_w$ = Inner wall temperature of pipe [°C or K]

- $T_b$ = Bulk temperature of molten salt [°C or K]

Nusslet co-relation to determine convective heat transfer (Amran et al, 2024):

$$h = (Nu*k/D) \tag{12}$$

$$Nu = 0.023 \cdot Re^{0.8} \cdot Pr^n \text{ (Nusslet number)} \tag{13}$$

$$R_e = (\rho*v*D/\psi). \text{ (Reynolds number)} \tag{14}$$

$$P_r = Cp*\psi/k \text{ (prandtl number)} \tag{15}$$

**Table 2: Dimensionless Flow Parameters and Heat Transfer Coefficient.**

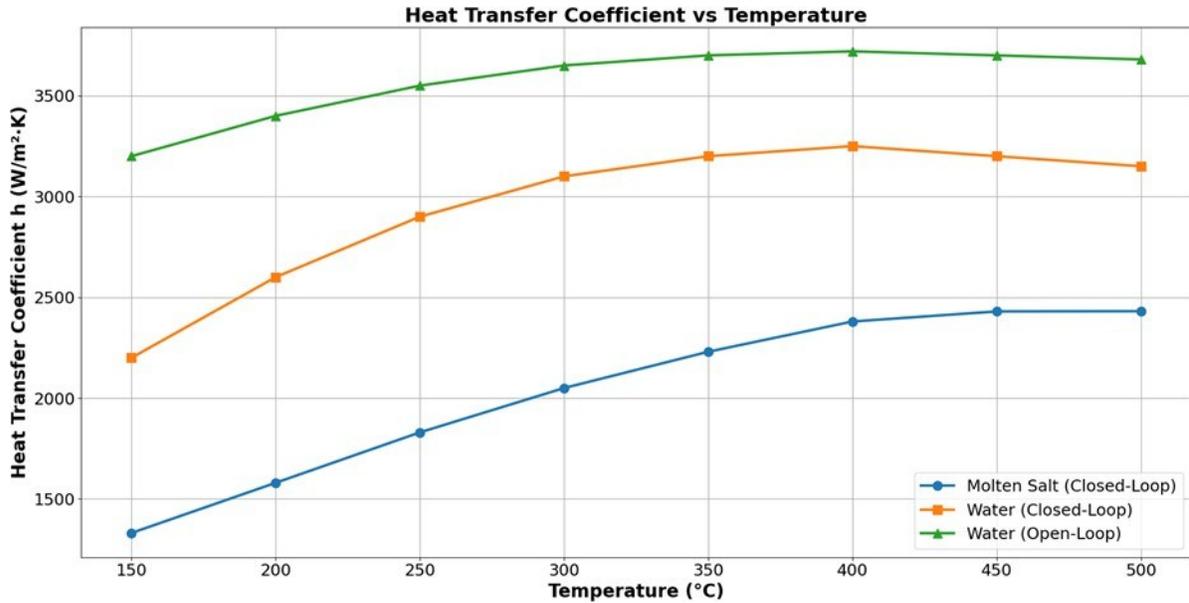| System characteristic | Values |
|---|---|
| Reynolds Number | 34500 (Turbulent flow) |
| Prandlt Number | 51.8 |
| Nusslet Number | 473 |
| Heat Transfer coefficient (h) | 2431 (w/m$^2$k) |



**Figure 3: comparison of Block ORC power and overall system efficiency between various Geothermal systems.**

The plot illustrates the variation of heat transfer coefficient with temperature for molten salt and water-based systems. Although water particularly in open-loop operation exhibits higher absolute heat transfer coefficients, molten salt demonstrates a consistent and stable increase in heat transfer performance across the temperature range. This behavior, combined with molten salt's high thermal stability and large heat capacity at elevated temperatures, enables it to retain and transport thermal energy more efficiently. As a result, molten salt is especially advantageous for high-temperature closed-loop systems where effective heat retention, reduced thermal losses, and stable long-term operation are critical (Ref. [6] McBay., 2012).

### 4. Thermal Drawdown Mitigation Strategies

Thermal drawdown in molten-salt closed-loop geothermal systems is mitigated through integrated geometric and operational design. High-temperature operation enables target power output at reduced heat-flux density, limiting near-well temperature decline. Multilateral and interconnected well geometries increase effective heat-exchange area and distribute thermal extraction across a larger rock volume. Coaxial flow configurations reduce internal thermal short-circuiting, preserving formation-to-fluid temperature gradients. Surface thermal storage further mitigates drawdown by decoupling heat extraction from continuous power generation over commercial lifetimes.

### 4.1. Heat extraction rate and role of overall thermal resistance

Equations (16) – (21) describe heat transfer from the geothermal formation to the working fluid using a thermal resistance network model. The extracted heat is calculated as the temperature difference between the formation and the fluid divided by the total thermal resistance, which is the sum of conduction resistances in the surrounding rock, cement, and pipe, along with the internal convective resistance. The logarithmic resistance terms arise from radial heat conduction in cylindrical layers, while the convective resistance accounts for heat transfer between the pipe wall and the circulating fluid. This approach is widely used for analyzing heat extraction in geothermal wellbore and borehole heat exchanger systems (Ref. [4] Koenig et al., 2015)

$$Q = (T_{formation} - T_{mol})/R_t \tag{16}$$

$$R_{total}' = R_{rock}' + R_{cement}' + R_{pipe}' + R_{conv}' \tag{17}$$

$$R\_rock^{'}(t) = 1/(2\pi k\_rock)\,ln_{fo}((r\_thermal(t))/r\_wellbore) \tag{18}$$

$$R\_pipe^{'} = 1/(2\pi k\_pipe)\,ln_{fo}(r\_(outer,pipe)/r\_(inner,pipe)) \tag{19}$$

$$R\_cement^{'} = 1/(2\pi k\_cement)\,ln_{fo}(r\_(outer,cement)/r\_(inner,cement)) \tag{20}$$

$$R\_conv^{'} = 1/(h\cdot(\pi D\_inner)) \tag{21}$$

$$rthermal(t) = 4\alpha t \tag{22}$$

**Table 3: Assumed material properties to estimate the Thermal resistances.**

| Material | Thermal Conductivity, k (W/m·K) | Source / Description |
|---|---|---|
| Rock (Granite) | 3.0 | Typical geothermal reservoir |
| Cement | 1.0 | well cement |
| Steel Pipe | 45.0 | Carbon steel |
| Molten Salt | 0.55 | Nitrate salt |

**Table 4: Thermal Barrier Analysis Results for Heat Flow Rate Estimation..**

| Parameter | Value | Units | Notes |
|---|---|---|---|
| R′_rock | 0.313 | m·K/W | Largest resistance |
| R′_cement | 0.0965 | m·K/W | Moderate |
| R′_pipe | 0.000305 | m·K/W | Negligible |
| R′_conv | 0.000852 | m·K/W | Very small |
| R′_total | 0.4107 | m·K/W | Dominated by rock |
| Q′ (per meter) | 852 | W/m | Heat flow rate |
| Q_calculated | 94.9 | kW | From resistances |

The calculated heat transfer from the surrounding rocks to the wellbore is relatively small and is strongly limited by the high thermal resistance of the formation, particularly the rock layer (Ref. [5] Zafar., 2024) This indicates that conductive heat inflow from the reservoir contributes only a minor portion of the total thermal energy extracted by the system. However, this result is beneficial when compared to conventional open-loop or fluid-dominated systems, as it confirms that the closed-loop wellbore design minimizes heat losses to the formation while relying primarily on the high heat capacity and thermal storage capability of the circulating molten salt. Consequently, thermal energy is retained within the system more efficiently, leading to stable and predictable power output without excessive dependence on continuous heat replenishment from the surrounding rocks.

**5. Molten-Salt Thermal Storage and Thermal Buffering**

Thermal energy storage in molten salt is a central feature of the proposed system. Molten salt serves simultaneously as the subsurface heat-transfer fluid and as the surface thermal storage medium, enabling direct buffering of extracted heat without intermediate phase change or conversion losses (Ref. [11] Yamamoto et al., 2020).

Thermal buffering allows heat to be extracted from the subsurface at a controlled, near-steady rate while power generation responds dynamically to grid demand. This decoupling reduces peak thermal gradients at the wellbore, improves long-term thermal sustainability, and increases the effective utilization of the geothermal resource (Ref. [8] Meenakshisundaram et al., 2025).

A further, system-level benefit arises from temporal decoupling of subsurface heat extraction and surface power production via molten-salt thermal storage. With storage, heat can be extracted at a controlled, near-steady rate while electricity output follows demand. The storage balance is simply

$$E_{store} = mc_p \Delta T$$

(23)

and the dispatch condition can be expressed as $\dot{Q}$ extract $\approx \langle \dot{Q}$ to power$\rangle$ over suitable averaging windows. This reduces peak thermal stress on the formation and converts a steady geothermal heat source into a dispatchable power asset without increasing instantaneous subsurface heat-flux demands.

In short, the concept leverages (i) the large thermal driving force of super-hot rock, (ii) conduction-governed predictability, and (iii) molten-salt sensible-heat buffering to achieve both drawdown mitigation and dispatchable generation in a physically transparent way.

Because molten salt remains thermally stable at super-hot rock temperatures, high-temperature storage can be maintained with minimal degradation, supporting dispatchable power generation over extended durations (Ref. [10] Man., 2021).

be repurposed into highly productive assets. In addition, many long-producing geothermal wells have experienced performance decline as brine deposition, scaling, mineral precipitation, or reservoir cooling reduced output to uneconomic levels. These wells can be re-engineered as closed-loop heat exchangers, bypassing the very permeability and fluid issues that caused

## 6. Economic Implications of Molten-Salt Thermal Buffering

Molten-salt thermal buffering improves closed-loop geothermal economics by decoupling heat extraction from electricity generation. Stored thermal energy can be dispatched during higher-value periods without increasing subsurface extraction, reducing curtailment, and increasing effective capacity factors (Ref. [15] YARA., tech sheet, no date) This enables participation in dispatchable grid services and improves overall revenue capture. In super-hot rock applications, the combination of high thermal input and storage materially outperforms non-buffered closed-loop systems (Ref. [9] Beckers et al., 2023). Thermal buffering also reduces upfront capital exposure and supports rapid scaling using existing global drilling inventories.

## 7. Levelized Cost of Electricity (LCOE)

LCOE is used here as a system-level benchmark representing the discounted lifetime cost per unit of electricity generated under consistent operating and financing assumptions and is applied solely for comparative evaluation against other firm generation technologies. For the 10 MW working field model pilot, total capital expenditure is conservatively estimated at approximately $50 million. This estimate explicitly includes worst-case drilling scenarios, including the potential need for new deep drilling into super-hot rock formations, and therefore represents an upper-bound cost appropriate for a first commercial demonstration rather than an expected steady-state deployment cost. Unlike conventional hydrothermal geothermal development, project viability does not depend on intersecting with a naturally permeable or productive reservoir. Any well drilled into sufficiently hot rock can be utilized for thermal extraction, materially reducing exploration risk and the probability of non-productive wells, and lowering effective drilling risk on a per-megawatt basis (Ref. [17] & [18] IRENA., 2024 & NREL., 2024). Operation and maintenance cost, with an ORC generator and standard geothermal maintenance, staffing, and compliance practices can be estimated at 2 - 4% of CAPEX per year. Standard variable cost can be estimated at $2 / MWh.

LCOE calculations assume a 20-year project life, consistent with the anticipated power purchase agreement (PPA), and a discount rate of 8%, reflecting early commercial geothermal financing practice.

$$\frac{\sum (I_t + M_t + F_t)/(1 + r)^i}{\sum E_t/(1 + r)^t}$$

(24)

- I = Initial Investment ($)

- M = Operation and Maintenance ($)

- F = Variable Cost ($)

- E = Total Generation (MWh)

- r = Discount Rate

$$\text{Capital recovery factor} = \frac{r(1+r)^n}{(1+r)^n - 1}$$

(25)

Under these modest assumptions, a newly drilled well yield the following LCOE and LCOH

| Parameter | Value | Units |
|---|---|---|
| Annual Net Electricity Generation | 95751.18 | MWh |
| Annual Net Heat Generation | 353169.036 | MWh |
| Capital Investment | 50000000 | $ |
| Fixed O&M Costs | 1500000 | $ |
| Variable Costs | 2 | $/MWh |
| Discount Rate | 0.08 | |
| Capital Recovery Factor | 0.102 | |
| LCOE | 70.929 | $/MWh |
| LCOH | 20.689 | $/MWh |
| Lifetime | 20 | Years |

## 8. Secondary Deployment Pathways

Molten-salt closed-loop systems can be deployed through retrofit of existing wells in addition to new super-hot rock developments (Ref. [6] McBay., 2012). Tens of millions of orphaned or abandoned oil and gas wells globally represent a large inventory of subsurface access drilled at substantial historical cost. Many intersect elevated-temperature formations or can be extended at far lower cost than new drilling. Sealed closed-loop conversion enables these assets to be repurposed as productive thermal infrastructure.

Similar opportunities exist in geothermal exploration and depleted production wells that encountered high temperatures but failed commercially due to permeability, chemistry, or pressure decline. Closed-loop operation relies on conductive heat transfer rather than formation of flow, enabling continued use of these wells. Collectively, these categories represent tens of thousands of near-term deployment sites.

## 9. Drilling Costs, Heat Capacity, and Economic Leverage at 375–550 °C

Conventional geothermal models assume drilling cost dominates capital expenditure and constrains LCOE, implicitly treating thermal output per well as fixed. However, LCOE is a ratio, and increasing energy delivered per well is as impactful as reducing drilling cost. In molten-salt closed-loop systems operating at 375–550 °C, per-well energy output increases substantially due to access to much higher rock heat and the high sensible heat capacity and thermal stability of molten salt. Under these conditions, drilling cost per megawatt delivered declines sharply even if drilling cost per meter remains unchanged.

This informs the deployment strategy. In super-hot formations, new wells are economically justified by order-of-magnitude increases in extractable heat, with potential outputs approaching 10–20 MW per well depending on depth and geometry. In lower-temperature settings, drilling is avoided by converting existing oil and gas or geothermal wells, yielding competitive LCOH and favorable LCOE from the reduced initial investment relative to the production life cycle. Molten-salt closed-loop geothermal thus shifts the economic focus from drilling cost reduction to maximizing thermal yield per well.

## 10. Conclusions

Molten-salt closed-loop geothermal systems engineered for super-hot rock environments offer a compelling and technically credible pathway to large-scale, dispatchable, zero-carbon energy generation. By intentionally targeting ultra-high-temperature resources while maintaining full hydraulic isolation from the surrounding formation, this class of system overcomes many of the fundamental limitations associated with conventional hydrothermal and enhanced geothermal approaches. In particular, it eliminates dependence on natural permeability, reduces subsurface uncertainty, and avoids fluid loss, induced seismicity, and reservoir degradation associated with open-loop systems.

A central advancement of the proposed approach lies in its deliberate management of thermal drawdown. Rather than maximizing short-term heat extraction at the expense of long-term performance, the system is designed to operate within controlled thermal gradients that preserve conductive heat replenishment from the surrounding rock mass. This strategy enables sustained heat recovery over multi-decadal operating periods, addressing one of the most persistent criticisms of closed-loop geothermal concepts - namely, the risk of rapid thermal depletion and declining output over time.

The integration of molten salt as the working heat-transfer and thermal storage medium further strengthens the system's technical and commercial viability. Molten salt enables efficient heat transport at temperatures well beyond the practical limits of water-based systems, while simultaneously providing intrinsic thermal buffering. This buffering decouples subsurface heat extraction from surface power conversion, allowing for stable, dispatchable output and improved capacity factors. The result is a geothermal system that behaves not only as a heat source, but also as a form of long-duration thermal energy storage.

From a systems perspective, the combination of ultra-high-temperature operation, closed-loop architecture, and thermal storage creates a flexible platform capable of supporting multiple end-use applications. These include high-efficiency power generation, industrial process heat, district heating, and hybrid integration with other energy systems. Importantly, the modular nature of the design enables scalability across a wide range of project sizes and geological settings, including the repurposing of existing deep wells where appropriate.

Taken together, these features address the principal technical objections historically raised against closed-loop geothermal systems, including limited heat extraction rates, poor long-term sustainability, and lack of dispatchability. The proposed molten-salt closed-loop architecture demonstrates that, when properly engineered, closed-loop geothermal can evolve from a niche concept into a robust, bankable energy technology. As super-hot rock resources are increasingly characterized worldwide, this approach offers a viable pathway for geothermal energy to contribute meaningfully to future low-carbon energy systems at commercial scale.

**REFERENCES**

[1] Hefni, M. A., Xu, M., Hassani, F., Ghoreishi-Madiseh, S. A., Ahmed, H. M., Saleem, H. A., … Sasmito, A. P. (2021). An analytical model for transient heat transfer with a time-dependent boundary in solar- and waste-heat-assisted geothermal borehole systems: From single to multiple boreholes. **Applied Sciences, 11**(21), 10338. https://doi.org/10.3390/app112110338.

[2] Ali, B. (2019). Sustainability assessment of power generation from an abandoned oil and gas well in Alberta, Canada. **Journal of Energy and Power Technology, 1**(3), 1–16. https://doi.org/10.21926/jept.1903002.

[3] Zarrouk, S. J., & Moon, H. (2014). Efficiency of geothermal power plants: A worldwide review. **Geothermics, 51**, 142–153. https://doi.org/10.1016/j.geothermics.2013.11.001.

[4] Koenig, A. A. (2015). Thermal resistance of borehole heat exchangers composed of multiple loops and custom shapes. **Geothermal Energy, 3**(1), Article 10. https://doi.org/10.1186/s40517-015-0029-1.

[5] Zafar, M., Sakidin, H., Sheremet, M., Dzulkarnain, I., Nazar, R. M., Hussain, A., Said, Z., Afzal, F., Al-Yaari, A., & Khan, M. S. (2024). A comprehensive review of mixed convection heat transfer through various Prandtl number fluids, geometries, and orientations. **Processes, 12**(12), 2749. https://doi.org/10.3390/pr12122749.

[6] McBay, David Alan, Closed-Loop Geothermal Energy Collection System, U.S. Patent **US 10,330,348 B2**, filed March 13, 2014, priority February 17, 2012, issued June 25, 2019. https://patents.google.com/patent/US9927151B2/en. https://patents.google.com/patent/US10605491B2/en.

[7] Meenakshisundaram, A., Tomomewo, O. S., Aimen, L., & Bade, S. O. (2024). A comprehensive analysis of repurposing abandoned oil wells for different energy uses: Exploration, applications, and repurposing challenges. Cleaner Engineering and Technology, 100797. https://doi.org/10.1016/j.clet.2024.100797

[8] Meenakshisundaram, A., Tomomewo, O.S., Crowell, J., Alamooti, M., & Bade, S.O. (2025). Experimental assessment of enhanced geothermal system potential of partially abandoned or dry oil wells in a sedimentary basin. Energy Geoscience, 6, 100436. https://doi.org/10.1016/j.engeos.2025.100436

[9] Beckers, Koenraad, Yaroslav Vasyliv, Gabriela A. Bran-Anleu, Mario Martinez, Chad Augustine, and Mark White. 2023. Tabulated Database of Closed-Loop Geothermal Systems Performance for Cloud-Based Technical and Economic Modeling of Heat Production and Electricity Generation: Preprint. Golden, CO: National Renewable Energy Laboratory. NREL/CP-5700-84979. https://www.nrel.gov/docs/fy23osti/84979.pdf.

[10] MAN Energy Solutions. (2021). Molten salt energy storage: Ensuring the reliability of renewable power generation with superior time flexibility. Augsburg, Germany: MAN Energy Solutions SE. Available from: https://www.man-es.com. Published November 2021.

McBay, Meenakshisundaram, Doueiri, Yamaguchi, Swenson, Putra, McBay

[11] Yamamoto, K., Domoto, K., Tobo, M., Kawamizu, T., Yamana, T., & Ota, Y. (2020). Thermal storage system to provide highly-efficient electric power resilience in the era of renewable energy. Mitsubishi Heavy Industries Technical Review, Vol. 57, No. 1, March 2020. Mitsubishi Heavy Industries, Ltd. https://www.mhi.com/technology/review/abstract-57-1-40

[12] Colp, J. L. (1982). Final report: Magma Energy Research Project. SAND82-2377, Sandia National Laboratories, Albuquerque, NM and Livermore, CA. Prepared for the U.S. Department of Energy. https://www.ogp.om/wp-content/uploads/2024/06/Magma-Energy-Project.pdf

[13] Clean Air Task Force (CATF). (2022). Superhot Rock Energy: A vision for firm, global zero-carbon energy. Updated November 2022. Clean Air Task Force, Boston, MA. https://www.catf.us/resource/superhot-rock-energy-a-vision-for-firm-global-zero-carbon-energy/

[14] Special Metals Corporation. 2005. INCONEL® Alloy 617. Publication No. SMC-029. Huntington, West Virginia: Special Metals Corporation. https://www.specialmetals.com inconel-alloy-617

[15] YARA GmbH & Co. KG. Thermo-physical properties of Yara MOST: Ternary molten salt based on CaNaK-nitrate. Dülmen, Germany: YARA GmbH & Co. KG. https://www.yara.com/industrial-nitrogen/solar-power-molten-salt/

[16] Vallourec. THERMOCASE® VIT – Geothermal: Optimizing geothermal heat efficiency. Vallourec New Energies, brochure/documentation. https://www.vallourec.com

[17] International Renewable Energy Agency (IRENA). *Renewable Power Generation Costs in 2024.* Abu Dhabi: IRENA, 2025. This report provides global overview of installed costs, O&M levels, capacity factors, and levelized cost benchmarks for renewable electricity technologies, including geothermal. https://www.irena.org/-/media/Files/IRENA/Agency/Publication/2025/Jul/IRENA_TEC_RPGC_in_2024_Summary_2025.pdf

[18] National Renewable Energy Laboratory (NREL). *2024 Annual Technology Baseline (ATB) Cost and Performance Data — Geothermal Electricity.* Golden, CO: National Renewable Energy Laboratory, 2024. The ATB datasets include standardized assumptions for CAPEX, fixed and variable operations & maintenance (O&M), capacity factors, and LCOE for geothermal power plants (hydrothermal and technology innovation scenarios). https://atb.nrel.gov/electricity/2024b/geothermal